Published in final edited form as:

Sci Transl Med. 2021 September 08; 13(610): eabd4811. doi:10.1126/scitranslmed.abd4811.

Chromosomal instability sensitizes patient breast tumors to multipolar divisions induced by paclitaxel

Christina M. Scribano[1], **Jun Wan**[2], **Karla Esbona**[3], **John B. Tucker**[4], **Amber Lasek**[5], **Amber S. Zhou**[1], **Lauren M. Zasadil**[1], **Ryan Molini**[5], **Jonathan Fitzgerald**[1], **Angela M. Lager**[6], **Jennifer J. Laffin**[6], **Kayla Correia-Staudt**[3], **Kari B. Wisinski**[3], **Amye J. Tevaarwerk**[3], **Ruth O'Regan**[3,†], **Stephanie M. McGregor**[7], **Amy M. Fowler**[8,9,13], **Richard J. Chappell**[10], **Tim S. Bugni**[11], **Mark E. Burkard**[3,12,13], **Beth A. Weaver**[5,12,13,*]

[1]Molecular and Cellular Pharmacology Graduate Training Program, University of Wisconsin, Madison, WI 53705, USA.

[2]Physiology Graduate Training Program, University of Wisconsin, Madison, WI 53705, USA.

[3]Department of Medicine, University of Wisconsin, Madison, WI 53705, USA.

[4]Cancer Biology Graduate Training Program, University of Wisconsin, Madison, WI 53705, USA.

[5]Department of Cell and Regenerative Biology, University of Wisconsin, Madison, WI 53705, USA.

[6]Wisconsin State Laboratory of Hygiene, Madison, WI 53705, USA.

[7]Department of Pathology and Laboratory Medicine, University of Wisconsin, Madison, WI 53705, USA.

[8]Department of Radiology, University of Wisconsin, Madison, WI 53792, USA.

[9]Department of Medical Physics, University of Wisconsin, Madison, WI 53705, USA.

[10]Department of Statistics, University of Wisconsin, Madison, WI 53705, USA.

[11]School of Pharmacy, University of Wisconsin, Madison, WI 53705, USA

[12]Department of Oncology/McArdle Laboratory for Cancer Research, University of Wisconsin, Madison, WI 53705, USA.

[13]Carbone Cancer Center, University of Wisconsin-Madison, Madison, WI 53705, USA.

[*]To whom correspondence should be addressed: Beth A. Weaver, University of Wisconsin - Madison, 1111 Highland Avenue, 6109 WIMR, Madison WI 53705-2275, Tel: (608) 263-5309, Fax: (608) 265-6905, baweaver@wisc.edu.

[†]Present address: Department of Medicine, University of Rochester, Rochester, NY 14642, USA.

Author contributions:

C.M.S., T.S.B., M.E.B., B.A.W. conceived and designed experiments. C.M.S., K.E., J.B.T., A.L., A.S.Z., L.M.Z., R.M., J.F., A.M.L., J.J.L., K.C-S., S.M.M., A.M.F. performed experiments, collected, and analyzed data. J.W. generated cell lines. K.B.W, A.J.T., R.O'R., and M.E.B enrolled patients. C.M.S., and R.J.C. performed statistical analysis. C.M.S. and B.A.W. wrote the manuscript. All authors reviewed the manuscript.

Competing interests:

M.E.B. declares the following: Medical advisory board of Strata Oncology; Research funding from Abbvie, Genentech, Puma, Arcus, Apollomics, Loxo Oncology/Lilly, and Elevation Oncology.

Data and materials availability: All data associated with this study are present in the paper or supplementary materials.

Abstract

Paclitaxel (Taxol) is a cornerstone of cancer treatment. However, its mechanism of cytotoxicity is incompletely understood and not all patients benefit. We discovered that breast cancer patients did not accumulate sufficient intratumoral paclitaxel to induce mitotic arrest. Instead, clinically relevant concentrations induced multipolar mitotic spindle formation. However, the extent of early multipolarity did not predict patient response. While multipolar divisions frequently led to cell death, multipolar spindles focused into bipolar spindles prior to division at variable frequency, and maintaining multipolarity throughout mitosis was critical to induce the high rates of chromosomal instability necessary for paclitaxel to elicit cell death. Increasing multipolar divisions in paclitaxel resulted in improved cytotoxicity. Conversely, decreasing paclitaxel-induced multipolar divisions reduced paclitaxel efficacy. Moreover, we discovered that pre-existing chromosomal instability sensitized breast cancer cells to paclitaxel. Both genetic and pharmacological methods of inducing chromosomal instability were sufficient to increase paclitaxel efficacy. In patients, pre-treatment chromosomal instability directly correlated with taxane response in metastatic breast cancer, such that patients with a higher rate of pre-existing chromosomal instability showed improved response to taxane. Together, these results support the use of baseline rates of chromosomal instability as a predictive biomarker for paclitaxel response. Furthermore, they suggest that agents that increase chromosomal instability or maintain multipolar spindles throughout mitosis will improve the clinical utility of paclitaxel.

One Sentence Summary:

Paclitaxel cytotoxicity in breast tumors depends on multipolar spindle maintenance and pre-existing chromosomal instability.

Introduction

Paclitaxel is the founding member of the taxane family of microtubule stabilizing drugs, and is used clinically as anti-mitotic chemotherapy to treat a variety of cancers, including breast, ovarian, and lung (1). In breast cancer, paclitaxel is a cornerstone of treatment and is used for primary and metastatic tumors of all subtypes (2). Paclitaxel can be administered preoperatively (neoadjuvant) or postoperatively (adjuvant) and is delivered as a single agent prior or subsequent to anthracycline chemotherapy (3). There are two standard-of-care dosing regimens for patients with primary breast cancer receiving paclitaxel therapy. Patients either receive four doses of 175 mg/m^2 paclitaxel every other week or 12 weekly doses of 80 mg/m^2 paclitaxel. The results of a large clinical trial (SWOG S0221) suggested that both regimens are equally effective (4). Similar doses and schedules are used in the metastatic cancer setting. However, only about 50% of breast cancer patients display tumor regression following paclitaxel treatment (5). There is currently no clinically used biomarker to predict patient response to paclitaxel, underscoring the importance of further mechanistic studies.

Despite the long history of paclitaxel use, its mechanism of therapeutic response remains controversial (6). A range of paclitaxel concentrations have been tested in cell culture, with most studies focusing on high concentrations that cause cell death due to mitotic arrest resulting from activation of the mitotic checkpoint [also known as the spindle assembly

checkpoint (7)]. It was widely assumed that mitotic arrest was necessary for the therapeutic action of paclitaxel; however, other drugs developed to cause mitotic arrest have been largely ineffective in patients due to an inadequate therapeutic window, including drugs targeting Aurora kinase A, Eg5/kinesin spindle protein, and Polo-like kinase 1 (6). Moreover, paclitaxel-induced mitotic arrest does not correlate with tumor response in preclinical allograft studies in mice (8) or in human breast cancer patients (9). These observations suggest that paclitaxel exerts antitumor effects through mechanisms other than unresolved mitotic arrest.

We recently discovered that breast cancer patients receiving 175 mg/m^2 paclitaxel have intratumoral concentrations of paclitaxel too low to cause mitotic arrest in patient tumors or cell models (10). High doses of paclitaxel (5 μM) cause supraphysiological intracellular drug concentrations and mitotic arrest, and increase the mitotic index ≥15 fold over baseline. In contrast, low nanomolar, clinically relevant concentrations of paclitaxel do not cause mitotic arrest and only increase the mitotic index ~3 fold (10). In all primary breast tumors examined, paclitaxel increased the percentage of multipolar, as distinct from normal bipolar, mitotic spindles (10). In cell culture, mitotic divisions on multipolar spindles resulted in a relatively brief mitotic delay, chromosome missegregation, aneuploid daughter cells, and increased cell death (10, 11). Thus, we proposed that paclitaxel exerts its anti-cancer effects by causing chromosome missegregation on multipolar spindles. In this study we address whether low-dose, weekly paclitaxel also induces multipolar spindles without mitotic arrest. Verifying this mechanism provides crucial insight necessary to elucidate why some tumors respond to paclitaxel, whereas others are resistant.

About 50% of breast tumors exhibit chromosomal instability, an ongoing rate of chromosome missegregation that generates heterogenous aneuploid cells (12, 13). The rate of chromosomal instability dictates cell viability (14-17). Low rates of chromosomal instability can be advantageous to tumor cells, since ongoing changes in genomic content provide variable karyotypes that allow cells to survive under various selective pressures (12, 18, 19). However, high rates of chromosomal instability cause cell death and tumor suppression, likely due to loss of both copies of an essential chromosome (20, 21) or the antiproliferative effects of aneuploidy-induced stress (22). In patients, high rates of chromosomal instability are associated with improved prognosis (23-25). Since 175 mg/m^2 paclitaxel induces multipolar spindles without mitotic arrest, and multipolar spindles elevate chromosomal instability (10, 11), we propose that paclitaxel exerts its anti-cancer effects by increasing chromosomal instability over a maximally tolerated threshold. Moreover, breast cancers that exhibit chromosomal instability prior to therapy may be poised to respond to the increase in chromosomal instability caused by paclitaxel.

Results

Both 80 mg/m^2 and 175 mg/m^2 paclitaxel result in similar intratumoral concentrations in primary breast cancers

To determine whether multipolar mitotic spindles without mitotic arrest were fundamental for the efficacy of paclitaxel and were therefore caused by 80 mg/m^2 as well as 175 mg/m^2 paclitaxel, we enrolled patients in an ongoing clinical trial in which patients with newly

diagnosed primary breast cancer were treated with standard-of-care weekly low-dose (80 mg/m^2) paclitaxel as a single agent. Enrolled patients were female with treatment naïve HER2-negative breast cancer, and consented to have timed research biopsies and blood tests. Patients with HER2-positive tumors were excluded from this study to eliminate the confounding variable of concurrent therapy with a HER2-targeted antibody. Data from the first 15 patients enrolled are reported here (ages 37-62, median 50; table S1). One patient withdrew from the study and three patients were evaluated for a subset of endpoints due to insufficient biopsy material (2) or deviation from treatment protocol (1).

The trial design is depicted in Fig. 1A. After diagnostic core needle biopsy, tumors were measured by ultrasound before patients received 12 weekly doses of 80 mg/m^2 paclitaxel infused over 1 hour. A second core biopsy and blood draw were obtained 20 hours after initiation of the first infusion of paclitaxel. This timepoint was selected because cultured breast cancer cells mount a robust mitotic arrest to high doses of paclitaxel at 20 hours, showing ≥15 fold increase in mitotic index as compared to vehicle-treated cells (10). Therefore, we expected that mitotic arrest would also be evident in patient tumors at 20 hours. After 12 doses of 80 mg/m^2 paclitaxel, tumors were measured again by ultrasound. Tumor response was evaluated by measurement of the largest tumor diameter at baseline and after paclitaxel therapy, according to Response Evaluation Criteria in Solid Tumors (RECIST) 1.1 guidelines (26). After paclitaxel treatment and tumor imaging, patients received 4 cycles of the DNA damaging drugs Adriamycin/doxorubicin and cyclophosphamide (AC) and surgery, with the order at the discretion of the treating physician.

Quantification of paclitaxel concentrations in patient samples revealed that intratumoral concentrations ranged from 0.34 to 3.43 μM 20 hours after the first dose of 80 mg/m^2 paclitaxel, which extends the lower limit of the clinically relevant range measured after 175 mg/m^2 paclitaxel [1.1-9.0 μM; Table 1, (10)]. Plasma concentrations of paclitaxel 20 hours after the first infusion ranged from 0.011 to 0.094 μM in our patient cohort (Table 1), in agreement with previous measurements (27) and similar to what was observed after 175 mg/m^2 paclitaxel (10). The degree of intratumoral accumulation of paclitaxel ranged from 9- to 172-fold (Table 1), consistent with its known uptake variability.

Mimicking the appropriate intratumoral concentration in cell lines was complicated by the fact that paclitaxel accumulates intracellularly to varying extents depending on the cell type and concentration used (10, 28, 29). Therefore, identifying the concentration of paclitaxel with which to treat cells in order to achieve a clinically relevant intracellular concentration required measurements over a range of concentrations in each cell line. Liquid chromatography followed by tandem mass spectrometry (LC-MS/MS) was used to identify clinically relevant ranges of paclitaxel in MDA-MB-231 triple negative breast cancer cells and MCF10A nontransformed breast epithelial cells, as well as in commonly used cellular models including HeLa cervical cancer cells and h-TERT immortalized retinal pigmented epithelial (RPE-1) cells (table S2). As expected based on previous results (10, 28, 29), the degree of intracellular paclitaxel concentration varied from 32-fold to 1360-fold based on cell type and the dose of paclitaxel administered. Low nanomolar doses of paclitaxel

recapitulated clinically relevant intracellular paclitaxel concentrations in each of these cell lines (table S2).

Paclitaxel induces multipolar spindles without mitotic arrest in primary breast cancer

To determine whether 80 mg/m^2 paclitaxel induces mitotic arrest or, like 175 mg/m^2 paclitaxel, multipolar mitotic spindles without mitotic arrest, tumor core biopsies acquired before and after paclitaxel therapy were analyzed by immunofluorescence (Fig. 1B). Before paclitaxel therapy, the majority of mitotic cells displayed a normal bipolar mitotic spindle (Fig. 1, B top and C). At 20 hours after 80 mg/m^2 paclitaxel treatment there was a substantial increase in multipolar mitotic cells in all patient cancers examined (Fig. 1, B bottom and C), with increases ranging from 25-60% (Fig. 1C, paired *t* test $p \leq 0.001$). This substantial increase in multipolar spindles was accompanied by only modest effects on the percentage of cells in mitosis (mitotic index; Fig. 1D). Thus, both standard doses of paclitaxel induce multipolar spindles without mitotic arrest in patient tumors.

Multipolar spindles induced by paclitaxel focus into bipolar spindles with variable frequency

Division of duplicated chromosomes into >2 daughter cells on a multipolar spindle typically results in massive chromosome missegregation and inviable progeny (11). However, multipolar spindles often focus into bipolar spindles prior to chromosome segregation, which reduces chromosome missegregation rates and increases cell viability (11). Because spindle pole focusing could not be assessed in patient samples, which are fixed specimens that contain an insufficient observed number of cells in late stages of mitosis for accurate analysis, the propensity of paclitaxel-induced multipolar spindles to focus into bipolar spindles was assessed in MDA-MB-231 and Cal51 cells. These cells were selected because they are human triple negative breast cancer cell lines that lack expression of the estrogen receptor (ER) and progesterone receptor (PR) and do not overexpress human epithelial growth factor receptor 2 (HER2). Treatment with 10 nM paclitaxel resulted in a clinically relevant intracellular concentration in both MDA-MB-231 and Cal51 cells [as well as in MCF10A, RPE1 and HeLa cells; table S2; (10)]. Henceforth, all experiments using paclitaxel are at clinically relevant concentrations unless otherwise noted.

Consistent with the effects in patient tumors, 10 nM paclitaxel caused a substantial increase in multipolar spindles without inducing the peak mitotic index caused by higher concentrations of drug in all 5 cell lines (Fig. 1E and F, S1A to G). However, these cell lines differed in their ability to maintain paclitaxel-induced multipolar spindles (Fig. 1G, S1H to M). The percentage of spindle multipolarity increased as cells progressed from early stages of mitosis (prometaphase and metaphase) to later stages (anaphase and telophase) in MDA-MB-231 cells (Fig. 1G) and remained largely unchanged in RPE1 and HeLa cells (fig. S1L and M). Whereas MDA-MB-231 (as well as RPE1 and HeLa) cells maintained multipolar spindles throughout division, Cal51 and MCF10A cells appeared to focus paclitaxel-induced multipolar spindles during mitotic transit (Fig. 1G, S1K).

Timelapse microscopy confirmed the propensity of Cal51 cells to focus paclitaxel-induced multipolar spindles (fig S1 H and I, movie S1 to S3). Cal51 cells expressing fluorescent α-

tubulin and histone H2B (from transgenes or after CRISPR-mediated tagging of endogenous loci) to visualize microtubules and chromosomes respectively, were observed in the presence or absence of 10 nM paclitaxel. Whereas control Cal51 cells had bipolar spindles at anaphase onset and formed two daughter cells, in the presence of a clinically relevant dose of paclitaxel, most cells exhibited a transient multipolar spindle in the early stages of mitosis and approximately 40% of cells had a multipolar spindle at anaphase onset (fig. S1H and I). Although over a third of cells entered anaphase with a multipolar spindle, continued spindle focusing coupled with partial cytokinesis failure produced two daughter cells in 95 ± 2% (range 93-96%) of divisions. While control-treated Cal51 cells showed the typical striking spindle elongation during anaphase (movie S1), multipolar spindle elongation in the presence of paclitaxel was often quite abbreviated (movie S2) and/or followed by rapid spindle focusing (movie S3), impeding identification of multipolar anaphase and telophase cells in fixed analysis. Thus, though fixed analysis underestimates anaphase/telophase multipolarity, timelapse analysis confirms that, unlike MDA-MB-231 cells, Cal51 cells readily focus paclitaxel-induced multipolar spindles into bipolar spindles.

Persistent multipolarity causes paclitaxel-induced cell death

Next, we performed timelapse microscopy to track the fate of paclitaxel-treated cells. We noted that mitotic arrest, which is followed by death during mitosis or mitotic slippage to produce a tetraploid G1 cell, occurred very rarely in cells treated with clinically relevant concentrations of paclitaxel. Of all cells observed here, mitotic slippage occurred in 4 of 1060 (0.38%), death from mitosis in 17 of 1060 (1.6%), and mitotic arrest with an unknown fate in 7 of 1060 (0.67%), while the remaining cells successfully transited mitosis and divided their chromosomes in anaphase after a relatively brief mitotic delay.

Given that the vast majority of cells successfully completed mitosis, we tracked the fate of daughter cells resulting from these divisions in DMSO-treated controls and in clinically relevant concentrations of paclitaxel using 72-hour timelapse microscopy. We categorized cells based on whether they exhibited only a normal bipolar spindle or at least transient multipolarity. Cells with multipolar spindles, whether transient or persistent, showed a higher frequency of daughter cell death than cells with only bipolar spindles (Fig. 1H). In order to determine if multipolar persistence led to cell death, cells with multipolar spindles were further subdivided based on the duration the multipolar spindle was maintained. Cells with the most persistent multipolar spindles maintained multipolarity throughout mitosis and produced three or more daughter cells. These divisions resulted in higher frequencies of daughter cell death than cells with a multipolar spindle that persisted until anaphase onset, but produced two daughter cells as a result of spindle pole focusing after anaphase onset and/or partial cytokinesis failure (Fig. 1H). These divisions resulted in higher frequencies of cell death than divisions with the lowest degree of multipolar persistence, which had a multipolar spindle in prometaphase that was subsequently focused into a bipolar spindle prior to anaphase onset and remained bipolar throughout anaphase and telophase to produce two daughter cells. Overall, multipolar divisions resulted in more cell death than bipolar divisions in both cell lines (Fig. 1H), although multipolar divisions were rarer in Cal51 cells compared to MDA-MB-231 cells due to their increased propensity to cluster multipolar spindles.

To disentangle the contributions of persistent multipolarity from the effects of a delayed mitosis on cytotoxicity, we treated MDA-MB-231 and Cal51 breast cancer cell lines and nontransformed breast epithelial MCF10A cells with concentrations of paclitaxel that yielded similar mitotic delays (fig. S2A). We found no significant difference in the duration of divisions that resulted in death of at least one daughter cell as compared to divisions that produced only viable daughter cells (fig. S2 B to D). When comparing multipolar spindle persistence and cell fate under these conditions, we again observed that multipolar divisions resulted in more cell death than bipolar divisions in all three cell lines (fig. S2E to G). Moreover, we found that multipolar spindles that were maintained longer in mitosis led to a higher rate of cell death compared to cells that focused multipolar spindles into bipolar spindles earlier in mitosis (fig. S2E to G). These data support the conclusion that persistent multipolarity that causes high rates of chromosome missegregation, rather than mitotic delay, is responsible for paclitaxel cytotoxicity.

Increasing multipolar divisions improves paclitaxel efficacy in breast cell lines

If chromosome division on multipolar spindles is important for the efficacy of paclitaxel, increasing paclitaxel-induced multipolar divisions should increase paclitaxel cytotoxicity. Two methods were used to increase multipolar divisions in Cal51 breast cancer cells, which readily cluster paclitaxel-induced multipolar spindles (Fig. 1G, S1, H and I). First, an inhibitor of the kinesin-like protein HSET/KifC1, which functions in spindle pole clustering in cells with and without centrosome amplification (30, 31), was used. Though Cal51 cells did not overexpress HSET (fig. S1J), inhibition of HSET activity with CW-069 (32) in the presence of paclitaxel was sufficient to increase multipolar spindles in late stages of mitosis without affecting early mitotic spindle polarity (Fig. 2, A to C, S3, A and B). Moreover, this combination substantially decreased cell viability and increased cell death when compared to cells treated with paclitaxel alone (Fig. 2, D and E, S3, C and D). Similar results were achieved with a second inhibitor of HSET, AZ82 (fig. S3, E to H).

As a second approach to increase multipolar divisions in paclitaxel, we genetically introduced centrosome amplification, which is known to induce at least transient multipolar spindles (11). For these experiments, we used nontransformed breast epithelial MCF10A cells, which have a low basal rate of centrosome amplification. Centrosome amplification was accomplished by tetracycline (tet)-inducible overexpression of Polo-like kinase 4 (Plk4), the master regulator of centriole duplication (33, 34). Overexpression of Plk4 produced centrosome amplification in a majority of cells over at least 10 days (fig. S4, A and B). In fixed cells, Plk4 overexpression increased multipolar spindles early in mitosis, but these had largely focused into bipolar spindles in anaphase and telophase cells (fig. S4, C to F). However, in a subclinical dose of paclitaxel (1 nM), centrosome amplification substantially increased the incidence of multipolar spindles both before and after anaphase onset, as compared to paclitaxel treatment alone (fig. S4, C to F). Timelapse analysis of MCF10A cells expressing histone H2B-mNeonGreen and mScarlet-tubulin (Fig. 3, A and B, movies S4 and S5) revealed that compared to paclitaxel treatment alone, centrosome amplification increased the incidence of multipolar spindles and the number of poles per spindle before (fig. S4, G and H), after (Fig. S4I), and at (Fig. 3C, S4J) anaphase onset. Importantly, death of cells treated with paclitaxel was dramatically increased by Plk4

overexpression and the resulting increase in multipolarity (Fig. 3, C to E). Although overall mitotic duration did not predict cell fate (fig. S4K), cells that spent more time after anaphase onset with multipolar spindles than bipolar spindles were particularly likely to die (Fig. 3E). Consistent with this, centrosome amplification substantially reduced the metabolic viability of parental MCF10A cells treated with a subclinical dose of paclitaxel (fig. S4L). Thus, increasing multipolar divisions via HSET inhibition or centrosome amplification sensitizes cells to paclitaxel.

Reducing multipolar divisions reduces paclitaxel cytotoxicity

If chromosome division on multipolar spindles is important for the efficacy of paclitaxel, reducing paclitaxel-induced multipolar divisions should decrease paclitaxel cytotoxicity. To test this, we used two strategies to reduce paclitaxel-induced spindle multipolarity in MDA-MB-231 human breast cancer cells, a majority of which underwent multipolar divisions when treated with clinically relevant concentrations of paclitaxel (Fig. 1G). The first strategy involved chemical inhibition of the kinase Monopolar spindles 1 (Mps1; also known as TTK). Multiple clinical trials aimed at determining whether Mps1 inhibition increases the efficacy of paclitaxel in solid tumors are currently ongoing (NCT03411161, NCT03328494, NCT02366949), providing a rationale to mechanistically examine this combination treatment. A pharmacological inhibitor of Mps1, reversine (35), reduced mitotic timing both in the absence and presence of paclitaxel (fig. S5A). Reversine treatment did not affect establishment of bipolar spindles in control cells or multipolar spindles in paclitaxel-treated cells (Fig. 4, A and B, S5B). However, inhibition of Mps1 substantially reduced the incidence of multipolar spindles in late stages of mitosis (Fig. 4A and C, S5C), suggesting that reversine impaired the maintenance of paclitaxel-induced multipolarity, permitting cells to form bipolar spindles. Timelapse microscopy of MDA-MB-231 cells expressing GFP-tubulin and RFP-histone H2B confirmed that Mps1 inhibition substantially reduced the number of spindle poles in MDA-MB-231 cells entering anaphase (Fig. 4D). Spindle poles continued to focus after initial chromosome separation at anaphase onset (fig. S5D), resulting in a substantial decrease in the number of daughter cells formed (Fig. 4E), including an increase in the formation of a single daughter cell from divisions in the combined treatment of paclitaxel and reversine (Fig. 4E). These single daughter cells almost exclusively resulted from spindle pole focusing after anaphase onset and/or cytokinesis failure, rather than from mitotic slippage, which was observed in only 2 of 224 (0.89%) of cells. Consistent with a reduction in multipolar divisions and in chromosome missegregation, reversine treatment increased metabolic survival and decreased cell death in cells treated with paclitaxel (Fig. 4, F and G). Whole genome doubling as a result of single daughter cell formation may contribute to the buffering of chromosome missegregation in the combination treatment. A second Mps1 inhibitor, AZ3146 (36), also increased metabolic survival and colony-forming ability in cells treated with paclitaxel (fig. S5, E and F), decreasing the likelihood that the reduction in paclitaxel efficacy was due to off-target effects of reversine.

A second method of reducing paclitaxel-induced multipolar divisions involved upregulation of the mitotic checkpoint protein Mitotic Arrest Deficient 1 (Mad1), which is frequently observed in breast cancer and is associated with poor patient prognosis (37). We generated

MDA-MB-231 breast cancer cells stably expressing tet-inducible Mad1-YFP (38). 24 hour tet treatment induced uniform, clinically relevant Mad1 upregulation [fig. S6, A and B, (37, 38)], which decreased the duration of mitosis (fig. S6C), without affecting the incidence of early mitotic spindle multipolarity in cells treated with paclitaxel (Fig. 5, A and B, S6D). However, Mad1-YFP expression substantially decreased the incidence of multipolar anaphase and telophase spindles in MDA-MB-231 cells treated with 10 nM paclitaxel (Fig. 5A and C, S6E) and reduced the number of daughter cells formed (Fig. 5D). While most divisions in MDA-MB-231 cells treated with paclitaxel produced 3 daughter cells, in paclitaxel-treated cells expressing Mad1-YFP most divisions resulted in 2 daughter cells (Fig. 5D). Although these divisions sometimes resulted in a single daughter cell, these single daughters exclusively resulted from spindle pole focusing after anaphase onset and/or cytokinesis failure, rather than from mitotic slippage, which was observed in 0 of 203 cells analyzed. Hence, Mad1 upregulation had no impact on multipolar spindle formation early in mitosis but reduced the maintenance of multipolar spindles in MDA-MB-231 cells, resulting in fewer multipolar divisions and reduced chromosomal instability. Importantly, when treated with 10 nM paclitaxel, cells expressing Mad1-YFP showed decreased cell death (Fig. 5E) and increased metabolic viability and colony formation (Fig. 5F and S6F) as compared to isogenic MDA-MB-231 cells without Mad1 upregulation.

Consistent with these results in cell culture, expression of Mad1-YFP reduced the paclitaxel sensitivity of orthotopic MDA-MB-231 tumors in athymic nude mice treated with a clinically relevant dose of paclitaxel every other day for 5 days once tumors reached a minimum volume of 75 mm^3 (1.19-2.28 μM after iv injection of 30 mg/kg paclitaxel; Fig. 5G, S6G). Tumors expressing Mad1-YFP were resistant to paclitaxel as compared to isogenic parental MDA-MB-231 cells with endogenous Mad1 expression. Whereas tumors expressing Mad1-YFP shrank by 31% over a period of 14 days and then grew to their original size by 18 days, parental tumors shrank by 53% over a period of 25 days and did not recover to their initial size given a period of 44 days (Fig. 5H, S6, H and I). Thus, reducing paclitaxel-induced multipolar divisions in MDA-MB-231 cells reduced chromosomal instability and decreased the cytotoxicity of paclitaxel in vitro and in vivo.

Pre-anaphase multipolarity is not predictive of paclitaxel patient response

Although cell culture experiments demonstrated that the maintenance of multipolar spindles in late stages of mitosis was critical for paclitaxel efficacy, patient samples cannot be assessed for multipolar spindle maintenance due to a lack of observed anaphase and telophase cells. In all patient samples, a large majority of mitotic cells identified both before and after paclitaxel treatment were in stages of mitosis prior to anaphase onset (96 +/− 4%, mean +/− SD, range 88%−100%). This precludes determination of the prevalence of multipolar spindle focusing in fixed biopsy specimens.

In our analysis of predominately pre-anaphase mitotic cells, neither the overall incidence of spindle multipolarity achieved in response to paclitaxel nor the percent increase in multipolar spindles were predictive of patient response (fig. S7, A to D), likely because these spindles in early stages of mitosis could be subsequently focused into bipolar spindles with varying efficiency. As in our previous patient cohort treated with 175 mg/m^2 paclitaxel

(10), response did not correlate with the intratumoral concentration of paclitaxel (fig. S7E). Ki67, which is used clinically as a measure of the proliferative ability of tumors, correlated with mitotic index (fig. S7F). However, neither pre-treatment Ki67 nor mitotic index before or after treatment correlated with tumor response (fig. S7, G to I) suggesting that, though a minimum amount of proliferation is likely necessary for paclitaxel response, above a minimal threshold of proliferation, additional factors dictate patient outcome. Thus, these characteristics are not sufficient to predict the response of individual tumors to paclitaxel and an additional metric(s) is necessary.

Chromosomal instability sensitizes breast cancer cells to paclitaxel

To test whether other mechanisms of chromosomal instability sensitize cells to paclitaxel, we increased chromosomal instability in Cal51 cells, which typically focus paclitaxel-induced multipolar spindles such that a majority of cells undergo bipolar divisions (Fig. 1G, S1, H and I), via two mechanisms. First, we inducibly upregulated Mad1-mNeonGreen (fig. S8, A to B). Whereas expression of Mad1 decreased chromosomal instability in paclitaxel-treated MDA-MB-231 cells by reducing the high percentage (>89%) of cells that underwent multipolar divisions (Fig. 1G, 5C), the incidence of multipolar divisions in paclitaxel-treated Cal51 cells was relatively low and unaffected by expression of Mad1-mNeonGreen (Fig. 6, A to C, S8, C and D). Although upregulation of Mad1 did not impact multipolar divisions in this cell type, it impaired mitotic checkpoint signaling which reduced mitotic timing and increased mitotic errors consistent with chromosome missegregation in the absence of paclitaxel, as expected (Fig. 6D, S8E). Expression of Mad1-mNeonGreen also increased mitotic defects indicative of chromosomal instability in the presence of paclitaxel in Cal51 cells (Fig. 6D). Defects during anaphase and telophase primarily occurred on bipolar spindles (fig. S8, F to H). This increase in chromosomal instability increased paclitaxel sensitivity; Cal51 cells expressing Mad1-mNeonGreen had decreased metabolic viability and colony forming ability and increased cell death in paclitaxel as compared to cells without Mad1-mNeonGreen (Fig. 6, E and F, S8, I and J). Similar results were observed in DLD1 cells, which also primarily exhibited bipolar divisions when treated with paclitaxel (fig. S8, K to M).

We also induced chromosomal instability by inhibition of the plus-end directed kinesin CENtromere associated Protein E (CENP-E) with GSK923295 (39). Timelapse microscopy of cells with endogenously labeled histone H2B-mScarlet and α-tubulin-mNeonGreen (Fig. 6, G to O) revealed that, as expected, control cells typically underwent a normal division (Fig. 6G), while CENP-E inhibition alone caused a substantial increase in misaligned chromosomes at or near spindle poles (Fig. 6H). 80% +/− 8.0% (mean +/− SEM) of cells treated with GSK923295 alone initially displayed misaligned chromosomes, though many of these ultimately aligned prior to anaphase onset (Fig. 6H and J to L). CENP-E inhibition did not affect the propensity of Cal51 cells to focus paclitaxel-induced multipolar spindles (Fig. 6M and N). It did, however, substantially increase the frequency with which cells entered anaphase with misaligned chromosomes, as well as the number of misaligned chromosomes at anaphase onset, which increased chromosomal instablility over paclitaxel treatment alone (Fig. 6I and J to L). In addition to increased chromosomal instability, treatment of cells with GSK923295 and paclitaxel also increased cell death (O). Importantly, a formal Chou-Talalay

synergy test (40) confirmed that CENP-E inhibition is synergistic with clinically relevant doses of paclitaxel (table S3). Thus, two mechanisms of increasing chromosomal instability (Mad1 upregulation and CENP-E inhibition) increased sensitivity to paclitaxel.

Pre-treatment chromosomal instability sensitizes metastatic breast cancer to taxane treatment

To investigate the effect of chromosomal instability on the sensitivity of patient cancers to paclitaxel, we followed these promising results in cell culture with a retrospective analysis of patient samples. We identified 37 cases of metastatic breast cancer with measurable disease and available archived tissue that were treated with single agent taxane therapy. Patients either received paclitaxel (16 cases), albumin-bound paclitaxel (nab-paclitaxel; 17 cases), or the paclitaxel analog docetaxel (4 cases). Patient characteristics are summarized in table S4. Response to taxane therapy was evaluated according to RECIST 1.1 guidelines [Fig. 7, A to C; (26)]. Rates of chromosomal instability prior to treatment were measured with interphase fluorescence in situ hybridization (FISH) using centromeric probes for 6 different chromosomes. Chromosomal instability was quantified by calculating the average percentage of non-modal chromosomes [Fig. 7D, supplementary methods, (13)]. Taxane response did not correlate with breast cancer receptor subtype (Fig. 7C) or several variables previously suggested to influence taxane sensitivity, including β-tubulin III and phospho-glycoprotein 1 (P-gp1) expression (fig. S9). Samples from metastatic tumors were available in 21 cases, 11 of which also had matching tissue from the primary site. Only primary tumor samples were available in 16 cases. When including both primary and metastatic samples, we observed a direct correlation between pre-treatment chromosomal instability and taxane response, such that cancers with higher rates of chromosomal instability before therapy responded preferentially to taxane treatment (Fig. 7E). This correlation plot yielded a slope of −0.71%, meaning for every percent increase in non-modal chromosomes, response to therapy improved by 0.71%. Removal of the cases containing samples from only primary tumors reduced the sample size but yielded a stronger correlation with a slope of −0.93% (Fig. 7F). These results demonstrate that, in this cohort, metastatic breast cancers with higher baseline rates of chromosomal instability experienced greater tumor shrinkage in response to taxane therapy.

Discussion

Paclitaxel remains a cornerstone of breast cancer treatment, even with the introduction of targeted therapy and immune checkpoint inhibitors. Prior to our work, it was largely accepted that paclitaxel exerts its anti-cancer effects by causing mitotic arrest, as it does at typically used concentrations in cell culture. It is now clear that neither standard-of-care paclitaxel treatment regimen produces an intratumoral concentration that is sufficient to arrest breast cancers in mitosis. Instead, contrary to the expectation of the last several decades, the anti-cancer effects of both doses of paclitaxel are due to chromosome missegregation on multipolar spindles and not mitotic arrest.

Our data further demonstrated that clustering of multipolar spindles represents a major mechanism of paclitaxel resistance, while drug efflux pumps do not. Paclitaxel accumulated

in all tumor samples at 9- to 172-fold the concentration found in plasma (Table 1) and induced multipolar spindles in all samples (Fig. 1C). No correlation was observed between intratumoral paclitaxel concentration and patient response (fig. S7E). These data support the conclusion that resistance is due to multipolar spindle focusing rather than reducing the intratumoral concentration of paclitaxel. Tumor cells exhibit varying capacities to focus paclitaxel-induced multipolar spindles (Fig. 1G and S1H to M). Previous experiments have established that daughter cells arising from multipolar divisions that produce more than two cells are often inviable and rarely continue to proliferate (11, 30). Paclitaxel-induced multipolar spindles can be focused into bipolar spindles throughout mitosis (Fig 1H, S2). However, increasing the duration of spindle multipolarity, particularly after anaphase onset, increased the likelihood of chromosome missegregation and cell death (Fig. 1H, 2 and 3, S2). Conversely, decreasing the time spindles spend in a multipolar state increased cell survival and decreased paclitaxel efficacy (Fig. 1H, 4, 5, S2). These data support the conclusion that multipolar spindle persistance contributes substantially to paclitaxel cytotoxicity. Consistent with this, down-regulation of the MTUS1 gene, which was associated with complete response to neoadjuvant chemotherapy that included taxane in three cohorts of breast cancer patients, increased the incidence of multipolar spindles in low-dose paclitaxel (41). Thus, treatments that prevent cells from focusing paclitaxel-induced multipolar spindles into bipolar spindles are likely to improve paclitaxel efficacy. In cells, inhibition of HSET increased multipolar spindle persistence and paclitaxel efficacy (Fig. 2, S3), but HSET inhibitors suitable for in vivo use are not yet available. Low amounts of replication stress have also been shown to increase the incidence of paclitaxel-induced multipolar divisions in cell culture, suggesting this may be a method of potentiating paclitaxel efficacy translatable to patient tumors (42).

Although efforts have been made to identify a biomarker for paclitaxel, none have been implemented in the clinic, in part due to a limited – and erroneous – understanding of the mechanism of paclitaxel. The importance of paclitaxel-induced multipolar spindles is their ability to induce chromosomal instability. Genetic or pharmacological insults that each cause low, tolerated rates of CIN can be combined to increase the rate of CIN over a maximally tolerated threshold (14-17, 43). Multipolar divisions result in missegregation of multiple chromosomes, typically more than bipolar divisions with lagging or misaligned chromosomes (11). However, in cells that focused paclitaxel-induced multipolar spindles into bipolar spindles, further increasing the rate of chromosomal instability effectively increased sensitivity to paclitaxel (Fig 6, table S3). Importantly, pre-treatment chromosomal instability correlated with response to taxane in metastatic breast cancer, even without determining the ability of individual tumors to focus paclitaxel-induced multipolar spindles (Fig 7). Thus, these data strongly support the utility of pre-treatment chromosomal instability as a predictive biomarker for paclitaxel response and suggest that treatments that increase the rate of chromosomal instability will increase response to paclitaxel.

Surprisingly, inhibition of Mps1 – which abrogates the mitotic checkpoint and causes chromosomal instability in otherwise unmanipulated cells – decreased chromosomal instability and cell death in MDA-MB-231 cells treated with clinically relevant concentrations of paclitaxel due to a decrease in multipolar divisions (Fig. 4, S5). Previous preclinical studies, which typically used high concentrations of paclitaxel we now recognize

to be above the clinically relevant range, have found that Mps1 inhibition sensitizes cells to paclitaxel (44, 45). Based on this, clinical trials aimed at determining whether Mps1 inhibition increases the efficacy of paclitaxel in solid tumors are ongoing (NCT03411161, NCT03328494, NCT02366949). It is possible that Mps1 inhibition will sensitize cancer cells that focus paclitaxel-induced multipolar spindles by increasing the rate of chromosomal instability on bipolar spindles, similar to what we observed with Mad1 upregulation in Cal51 and DLD1 cells and CENP-E inhibition in Cal51 cells (Fig. 6, S8, table S3). However, the variability in spindle focusing among cancers may present an unexpected challenge when combining Mps1 inhibitors with paclitaxel that prevents this approach from being uniformly successful.

We previously showed that Mad1 upregulation causes resistance to high concentrations of microtubule poisons, including paclitaxel, that cause mitotic arrest (37). We now understand that these concentrations are supraphysiological. At clinically relevant doses of paclitaxel, the differential impact of Mad1 upregulation on paclitaxel sensitivity in Cal51 and MDA-MB-231 cells was initially surprising. The differing ability of these cell lines to focus paclitaxel-induced multipolar spindles offers a unifying explanation, in which Mad1 upregulation increases chromosomal instability in paclitaxel-treated Cal51 cells but decreases chromosomal instability in paclitaxel-treated MDA-MB-231 cells (Fig. 5, 6). Discovery of the cell-intrinsic mechanisms used to focus paclitaxel-induced multipolar spindles is an important area for future research that will permit further mechanistic insight.

There are several limitations to our study. Our primary cohort is relatively young (median age 50), in part due to a relatively high proportion of triple negative patients, and consists of predominately white, non-Hispanic or Latino patients. The retrospective metastatic study was underpowered to validate a predictive biomarker and chromosomal instability does not explain all of the patient-to-patient variation in response in this cohort. We have considered three possible explanations. First, this may be because of modifying roles of other factors, including proliferation rate, p-glycoprotein, and β-tubulin III expression, though we did not find that these correlated with response in our dataset (fig. S9). Multipolar spindle clustering is likely to be a key additional factor in determining taxane response that could be used to improve a chromosomal instability-based biomarker. Given that centrosome amplification increased maintenance of paclitaxel-induced multipolar spindles in MCF10A cells (Fig. 3), centrosome amplification prior to therapy may impair focusing of paclitaxel-induced multipolar spindles and provide an additional predictor of response. Our recently developed method to quantitate centrosome amplification in circulating tumor cells from metastatic breast cancer patients (46) may be useful in this regard. Second, FISH is limited by sampling errors, sectioning artifacts, and analysis of only a subset of chromosomes. In the future, more comprehensive measures of cell-to-cell variation in chromosomes, like single-cell sequencing, may provide more accurate measures of chromosomal instability. Third, in this retrospective study, we were unable to control for prior treatments, site of biopsy, type of taxane used, and other sources of biologic variation such as breast cancer subtype or hormone receptor status. Therefore, we regard this as proof-of-principle that chromosomal instability relates to taxane reponse which accords with the laboratory experiments and mechanistic insights obtained from timed tumor biopsies after paclitaxel. Future studies

of a larger homogenous cohort of patients will permit a more robust test of chromosomal instability as a predictive biomarker.

In conclusion, paclitaxel uniformly increases multipolar spindles in breast cancers. Focusing of paclitaxel-induced multipolar spindles is a major mechanism of paclitaxel resistance, and identification of agents that maintain paclitaxel-induced multipolarity is of high priority to improve the clinical utility of paclitaxel. Cancers with a pre-existing rate of chromosomal instability are more sensitive to taxanes than chromosomally stable cancers, and our findings provide support that pre-treatment chromosomal instability can be used as a predictive biomarker of paclitaxel response. Such a biomarker would substantially improve patient outcomes by sparing non-responders paclitaxel-associated toxicities and reducing delays in receiving effective treatment.

Materials and Methods

Study Design

This is an ongoing study of the mechanism of paclitaxel in human breast cancer. The objectives were to determine clinically relevant paclitaxel concentrations and their effects on mitosis, chromosomal instability, cell proliferation, and response to treatment. These objectives were addressed by measurement of intratumoral and intracellular paclitaxel concentrations, immunofluorescence analysis of patient biopsies and cell lines treated with clinically relevant concentrations of paclitaxel (unless otherwise noted), orthotopic studies, FISH, and quantification of patient response according to RECIST 1.1 guidelines (26). All data presented here have been replicated in three mice (six tumors) or in 2-5 biological replicates for cell culture experiments. The patient sample size was selected to provide a sufficient number of biopsies for sampling intratumoral drug concentrations, effects on mitosis, cell-to-cell variation in chromosome copy number, and patient response. Fixed data analysis was blinded by concealment of slide labels. Cell samples and mice were assigned randomly to experimental groups. Data collection for each experiment is detailed in the respective figures, figure legends, and methods. Data for experiments where $n < 20$ are included in data file S1.

80 mg/m^2 paclitaxel study

Patients who volunteered to participate in the 80mg/m^2 paclitaxel study were enrolled in a prospective trial at the UW Carbone Cancer Center specifying the treatment, biopsy, and analysis plan. The protocol was approved by UW Health Sciences Institutional Review Board, ID 2016-1489, assigned UWCCC protocol number UW16106, conducted in accordance with the ethical standards established in the 1964 Declaration of Helsinki and registered on clinicaltrials.gov (NCT03096418). Patients were enrolled if they had previously untreated locally advanced breast cancer for which neoadjuvant chemotherapy was indicated. Subjects received four cycles of 80 mg/m^2 paclitaxel, per standard-of-care, with biopsy and treatment as outlined in Fig. 1A. A research biopsy was obtained 18–22 hours after start of the first infusion. After four cycles of paclitaxel, follow-up ultrasound imaging was performed to assess response to therapy and patients continued with surgery and anthracycline-based chemotherapy, per physician discretion. Data analysts were blinded

from patient response information until the study was completed and all data had been collected. Patient response was evaluated by an independent board-certified breast imaging radiologist who was blinded from the results of the study objectives. One patient withdrew and 3 patients were excluded from specific endpoints because of insufficient sample collected by biopsy (2) or deviation from treatment protocol (1). There were no major complications from protocol-mandated research biopsy.

Metastatic taxane study

We identified patients who were treated with a taxane-based regimen for metastatic breast cancer and then identified those with measurable disease. For these cases, response to taxanes was assessed by manual review of CT imaging following RECIST 1.1 criteria (26). Next, all cases with available archived tissue were identified and selected for analysis of potential biomarkers of paclitaxel as described. The protocol was approved through waiver of consent by UW Health Sciences Institutional Review Board, ID 2015-1584, assigned UWCCC protocol number UW15089, and conducted in accordance with the ethical standards established in the 1964 Declaration of Helsinki.

Statistical Analysis

Statistical analysis was performed using GraphPad Prism, R, or Mstat 6.4.2 software (http://www.mcardle.wisc.edu/mstat/index.html). Student's *t*-tests (two-tailed) were used to assess significance, unless otherwise noted. The Sen-Adichie test for parallelism was used for MTT assay growth curves (Fig. 2D, 4F, 5F, 6E and S4L) and mouse orthotopic growth curves (Fig. 5H, S6H-I), Wilcoxon rank sum test was used in Fig. 3E, a Mann-Whitney test was used in Fig. S8J, and simple linear regression was used for correlation plots (fig. S7C-I). The lines in Fig. 7 and S9 were fit using least squares regression in the R computing language, version 3.6.3. Other statistical parameters including the number of cells analyzed and the number of replicates are reported in the respective figure legends.

Supplementary Material

Refer to Web version on PubMed Central for supplementary material.

Acknowledgments:

We thank Heather Green in the UWCCC 3P lab core facility and Cameron Scarlett in the School of Pharmacy mass spectrometry facility for their assistance with paclitaxel measurements, Jessica Muszynski in the BRMS core for performing orthotopic experiments, Toshi Kinoshita in the Translational Research Initiatives in Pathology (TRIP) lab for histology services, Dr. Duane Compton for NuMA antibody, Dr. David Pellman for the inducible Plk4 MCF10A cell line, Dr. Theodorus Gadella for mScarlet (47), our patients for their participation in this research, and members of the Weaver, Burkard, and Suzuki laboratories for insightful discussions.

Funding:

This work was supported, in part, by University of Wisconsin Carbone Cancer Center Support Grant P30 CA014520, the Department of Pathology and Laboratory Medicine, Department of Defense grants W81XWH-16-1-0049 (B.A.W.) and W81XWH-16-1-0050 (M.E.B.), National Institutes of Health grants R01CA234904 (B.A.W., M.E.B.), R01GM104192 (T.S.B.), T32 CA009135 (C.M.S.), T32 GM008688 (J.F., A.S.Z.), Amerian Cancer Society Research Scholar Grant RSG-15-006-01-CCG (B.A.W.), and American Heart Association fellowship 16PRE29650011 (J.W.).

References:

1. Huang TC, Campbell TC, Comparison of weekly versus every 3 weeks paclitaxel in the treatment of advanced solid tumors: a meta-analysis. Cancer Treat Rev 38, 613–617 (2012). [PubMed: 22155063]
2. Crown J, O'Leary M, Ooi WS, Docetaxel and paclitaxel in the treatment of breast cancer: a review of clinical experience. Oncologist 9 Suppl 2, 24–32 (2004). [PubMed: 15161988]
3. Zaheed M, Wilcken N, Willson ML, O'Connell DL, Goodwin A, Sequencing of anthracyclines and taxanes in neoadjuvant and adjuvant therapy for early breast cancer. Cochrane Database Syst Rev 2, Cd012873 (2019). [PubMed: 30776132]
4. Budd GT, Barlow WE, Moore HC, Hobday TJ, Stewart JA, Isaacs C, Salim M, Cho JK, Rinn KJ, Albain KS, Chew HK, Burton GV, Moore TD, Srkalovic G, McGregor BA, Flaherty LE, Livingston RB, Lew DL, Gralow JR, Hortobagyi GN, SWOG S0221: a phase III trial comparing chemotherapy schedules in high-risk early-stage breast cancer. J Clin Oncol 33, 58–64 (2015). [PubMed: 25422488]
5. Fountzilas G, Dafni U, Dimopoulos MA, Koutras A, Skarlos D, Papakostas P, Gogas H, Bafaloukos D, Kalogera-Fountzila A, Samantas E, Briasoulis E, Pectasides D, Maniadakis N, Matsiakou F, Aravantinos G, Papadimitriou C, Karina M, Christodoulou C, Kosmidis P, Kalofonos HP, A randomized phase III study comparing three anthracycline-free taxane-based regimens, as first line chemotherapy, in metastatic breast cancer: a Hellenic Cooperative Oncology Group study. Breast Cancer Res Treat 115, 87–99 (2009). [PubMed: 18483853]
6. Komlodi-Pasztor E, Sackett DL, Fojo T, Tales of how great drugs were brought down by a flawed rationale--response. Clin Cancer Res 19, 1304 (2013). [PubMed: 23393076]
7. Waters JC, Chen RH, Murray AW, Salmon ED, Localization of Mad2 to kinetochores depends on microtubule attachment, not tension. J Cell Biol 141, 1181–1191 (1998). [PubMed: 9606210]
8. Milross CG, Mason KA, Hunter NR, Chung WK, Peters LJ, Milas L, Relationship of mitotic arrest and apoptosis to antitumor effect of paclitaxel. J Natl Cancer Inst 88, 1308–1314 (1996). [PubMed: 8797771]
9. Symmans WF, Volm MD, Shapiro RL, Perkins AB, Kim AY, Demaria S, Yee HT, McMullen H, Oratz R, Klein P, Formenti SC, Muggia F, Paclitaxel-induced apoptosis and mitotic arrest assessed by serial fine-needle aspiration: implications for early prediction of breast cancer response to neoadjuvant treatment. Clin Cancer Res 6, 4610–4617 (2000). [PubMed: 11156210]
10. Zasadil LM, Andersen KA, Yeum D, Rocque GB, Wilke LG, Tevaarwerk AJ, Raines RT, Burkard ME, Weaver BA, Cytotoxicity of paclitaxel in breast cancer is due to chromosome missegregation on multipolar spindles. Sci Transl Med 6, 229ra243 (2014).
11. Ganem NJ, Godinho SA, Pellman D, A mechanism linking extra centrosomes to chromosomal instability. Nature 460, 278–282 (2009). [PubMed: 19506557]
12. Zasadil LM, Britigan EM, Weaver BA, 2n or not 2n: Aneuploidy, polyploidy and chromosomal instability in primary and tumor cells. Semin Cell Dev Biol 24, 370–379 (2013). [PubMed: 23416057]
13. Denu RA, Zasadil LM, Kanugh C, Laffin J, Weaver BA, Burkard ME, Centrosome amplification induces high grade features and is prognostic of worse outcomes in breast cancer. BMC Cancer 16, 47 (2016). [PubMed: 26832928]
14. Silk AD, Zasadil LM, Holland AJ, Vitre B, Cleveland DW, Weaver BA, Chromosome missegregation rate predicts whether aneuploidy will promote or suppress tumors. Proc Natl Acad Sci U S A 110, E4134–4141 (2013). [PubMed: 24133140]
15. Weaver BA, Silk AD, Montagna C, Verdier-Pinard P, Cleveland DW, Aneuploidy acts both oncogenically and as a tumor suppressor. Cancer Cell 11, 25–36 (2007). [PubMed: 17189716]
16. Godek KM, Venere M, Wu Q, Mills KD, Hickey WF, Rich JN, Compton DA, Chromosomal Instability Affects the Tumorigenicity of Glioblastoma Tumor-Initiating Cells. Cancer Discov 6, 532–545 (2016). [PubMed: 27001151]
17. Laucius CD, Orr B, Compton DA, Chromosomal instability suppresses the growth of K-Ras-induced lung adenomas. Cell Cycle 18, 1702–1713 (2019). [PubMed: 31179849]

18. Selmecki AM, Dulmage K, Cowen LE, Anderson JB, Berman J, Acquisition of aneuploidy provides increased fitness during the evolution of antifungal drug resistance. PLoS Genet 5, e1000705 (2009). [PubMed: 19876375]
19. Rutledge SD, Douglas TA, Nicholson JM, Vila-Casadesús M, Kantzler CL, Wangsa D, Barroso-Vilares M, Kale SD, Logarinho E, Cimini D, Selective advantage of trisomic human cells cultured in non-standard conditions. Sci Rep 6, 22828 (2016). [PubMed: 26956415]
20. Funk LC, Wan J, Ryan SD, Kaur C, Sullivan R, Roopra A, Weaver BA, p53 is not required for cell death and tumor suppression caused by high chromosomal instability. Mol Cancer Res, (2020).
21. Kops GJ, Foltz DR, Cleveland DW, Lethality to human cancer cells through massive chromosome loss by inhibition of the mitotic checkpoint. Proc Natl Acad Sci U S A 101, 8699–8704 (2004). [PubMed: 15159543]
22. Chunduri NK, Storchová Z, The diverse consequences of aneuploidy. Nature Cell Biology 21, 54–62 (2019). [PubMed: 30602769]
23. Birkbak NJ, Eklund AC, Li Q, McClelland SE, Endesfelder D, Tan P, Tan IB, Richardson AL, Szallasi Z, Swanton C, Paradoxical relationship between chromosomal instability and survival outcome in cancer. Cancer Res 71, 3447–3452 (2011). [PubMed: 21270108]
24. Roylance R, Endesfelder D, Gorman P, Burrell RA, Sander J, Tomlinson I, Hanby AM, Speirs V, Richardson AL, Birkbak NJ, Eklund AC, Downward J, Kschischo M, Szallasi Z, Swanton C, Relationship of extreme chromosomal instability with long-term survival in a retrospective analysis of primary breast cancer. Cancer Epidemiol Biomarkers Prev 20, 2183–2194 (2011). [PubMed: 21784954]
25. Jamal-Hanjani M, A'Hern R, Birkbak NJ, Gorman P, Grönroos E, Ngang S, Nicola P, Rahman L, Thanopoulou E, Kelly G, Ellis P, Barrett-Lee P, Johnston SR, Bliss J, Roylance R, Swanton C, Extreme chromosomal instability forecasts improved outcome in ER-negative breast cancer: a prospective validation cohort study from the TACT trial. Ann Oncol 26, 1340–1346 (2015). [PubMed: 26003169]
26. Eisenhauer EA, Therasse P, Bogaerts J, Schwartz LH, Sargent D, Ford R, Dancey J, Arbuck S, Gwyther S, Mooney M, Rubinstein L, Shankar L, Dodd L, Kaplan R, Lacombe D, Verweij J, New response evaluation criteria in solid tumours: revised RECIST guideline (version 1.1). Eur J Cancer 45, 228–247 (2009). [PubMed: 19097774]
27. Hertz DL, Kidwell KM, Vangipuram K, Li F, Pai MP, Burness M, Griggs JJ, Schott AF, Van Poznak C, Hayes DF, Lavoie Smith EM, Henry NL, Paclitaxel Plasma Concentration after the First Infusion Predicts Treatment-Limiting Peripheral Neuropathy. Clin Cancer Res 24, 3602–3610 (2018). [PubMed: 29703818]
28. Yvon AM, Wadsworth P, Jordan MA, Taxol suppresses dynamics of individual microtubules in living human tumor cells. Mol Biol Cell 10, 947–959 (1999). [PubMed: 10198049]
29. Jordan MA, Wendell K, Gardiner S, Derry WB, Copp H, Wilson L, Mitotic block induced in HeLa cells by low concentrations of paclitaxel (Taxol) results in abnormal mitotic exit and apoptotic cell death. Cancer Res 56, 816–825 (1996). [PubMed: 8631019]
30. Kwon M, Godinho SA, Chandhok NS, Ganem NJ, Azioune A, Thery M, Pellman D, Mechanisms to suppress multipolar divisions in cancer cells with extra centrosomes. Genes Dev 22, 2189–2203 (2008). [PubMed: 18662975]
31. Kleylein-Sohn J, Pöllinger B, Ohmer M, Hofmann F, Nigg EA, Hemmings BA, Wartmann M, Acentrosomal spindle organization renders cancer cells dependent on the kinesin HSET. J Cell Sci 125, 5391–5402 (2012). [PubMed: 22946058]
32. Watts CA, Richards FM, Bender A, Bond PJ, Korb O, Kern O, Riddick M, Owen P, Myers RM, Raff J, Gergely F, Jodrell DI, Ley SV, Design, synthesis, and biological evaluation of an allosteric inhibitor of HSET that targets cancer cells with supernumerary centrosomes. Chem Biol 20, 1399–1410 (2013). [PubMed: 24210220]
33. Godinho SA, Picone R, Burute M, Dagher R, Su Y, Leung CT, Polyak K, Brugge JS, Théry M, Pellman D, Oncogene-like induction of cellular invasion from centrosome amplification. Nature 510, 167–171 (2014). [PubMed: 24739973]
34. Habedanck R, Stierhof YD, Wilkinson CJ, Nigg EA, The Polo kinase Plk4 functions in centriole duplication. Nat Cell Biol 7, 1140–1146 (2005). [PubMed: 16244668]

35. Santaguida S, Tighe A, D'Alise AM, Taylor SS, Musacchio A, Dissecting the role of MPS1 in chromosome biorientation and the spindle checkpoint through the small molecule inhibitor reversine. J Cell Biol 190, 73–87 (2010). [PubMed: 20624901]
36. Hewitt L, Tighe A, Santaguida S, White AM, Jones CD, Musacchio A, Green S, Taylor SS, Sustained Mps1 activity is required in mitosis to recruit O-Mad2 to the Mad1-C-Mad2 core complex. J Cell Biol 190, 25–34 (2010). [PubMed: 20624899]
37. Ryan SD, Britigan EM, Zasadil LM, Witte K, Audhya A, Roopra A, Weaver BA, Up-regulation of the mitotic checkpoint component Mad1 causes chromosomal instability and resistance to microtubule poisons. Proc Natl Acad Sci U S A 109, E2205–2214 (2012). [PubMed: 22778409]
38. Wan J, Block S, Scribano CM, Thiry R, Esbona K, Audhya A, Weaver BA, Mad1 destabilizes p53 by preventing PML from sequestering MDM2. Nat Commun 10, 1540 (2019). [PubMed: 30948704]
39. Wood KW, Lad L, Luo L, Qian X, Knight SD, Nevins N, Brejc K, Sutton D, Gilmartin AG, Chua PR, Desai R, Schauer SP, McNulty DE, Annan RS, Belmont LD, Garcia C, Lee Y, Diamond MA, Faucette LF, Giardiniere M, Zhang S, Sun CM, Vidal JD, Lichtsteiner S, Cornwell WD, Greshock JD, Wooster RF, Finer JT, Copeland RA, Huang PS, Morgans DJ, Dhanak D, Bergnes G, Sakowicz R, Jackson JR, Antitumor activity of an allosteric inhibitor of centromere-associated protein-E. Proc Natl Acad Sci U S A 107, 5839–5844 (2010). [PubMed: 20167803]
40. Chou TC, Drug combination studies and their synergy quantification using the Chou-Talalay method. Cancer Res 70, 440–446 (2010). [PubMed: 20068163]
41. Rodrigues-Ferreira S, Nehlig A, Moindjie H, Monchecourt C, Seiler C, Marangoni E, Chateau-Joubert S, Dujaric M-E, Servant N, Asselain B, de Cremoux P, Lacroix-Triki M, Arnedos M, Pierga J-Y, Andrá F, Nahmias C, Improving breast cancer sensitivity to paclitaxel by increasing aneuploidy. Proceedings of the National Academy of Sciences 116, 23691–23697 (2019).
42. Wilhelm T, Olziersky AM, Harry D, De Sousa F, Vassal H, Eskat A, Meraldi P, Mild replication stress causes chromosome mis-segregation via premature centriole disengagement. Nat Commun 10, 3585 (2019). [PubMed: 31395887]
43. Funk LC, Zasadil LM, Weaver BA, Living in CIN: Mitotic Infidelity and Its Consequences for Tumor Promotion and Suppression. Dev Cell 39, 638–652 (2016). [PubMed: 27997823]
44. Jemaè M, Galluzzi L, Kepp O, Senovilla L, Brands M, Boemer U, Koppitz M, Lienau P, Prechtl S, Schulze V, Siemeister G, Wengner AM, Mumberg D, Ziegelbauer K, Abrieu A, Castedo M, Vitale I, Kroemer G, Characterization of novel MPS1 inhibitors with preclinical anticancer activity. Cell Death Differ 20, 1532–1545 (2013). [PubMed: 23933817]
45. Wengner AM, Siemeister G, Koppitz M, Schulze V, Kosemund D, Klar U, Stoeckigt D, Neuhaus R, Lienau P, Bader B, Prechtl S, Raschke M, Frisk AL, von Ahsen O, Michels M, Kreft B, von Nussbaum F, Brands M, Mumberg D, Ziegelbauer K, Novel Mps1 Kinase Inhibitors with Potent Antitumor Activity. Mol Cancer Ther 15, 583–592 (2016). [PubMed: 26832791]
46. Singh A, Denu RA, Wolfe SK, Sperger JM, Schehr J, Witkowsky T, Esbona K, Chappell RJ, Weaver BA, Burkard ME, Lang JM, Centrosome amplification is a frequent event in circulating tumor cells from subjects with metastatic breast cancer. Mol Oncol, (2020).
47. Bindels DS, Haarbosch L, van Weeren L, Postma M, Wiese KE, Mastop M, Aumonier S, Gotthard G, Royant A, Hink MA, Gadella TW, mScarlet: a bright monomeric red fluorescent protein for cellular imaging. Nat Methods 14, 53–56 (2017). [PubMed: 27869816]

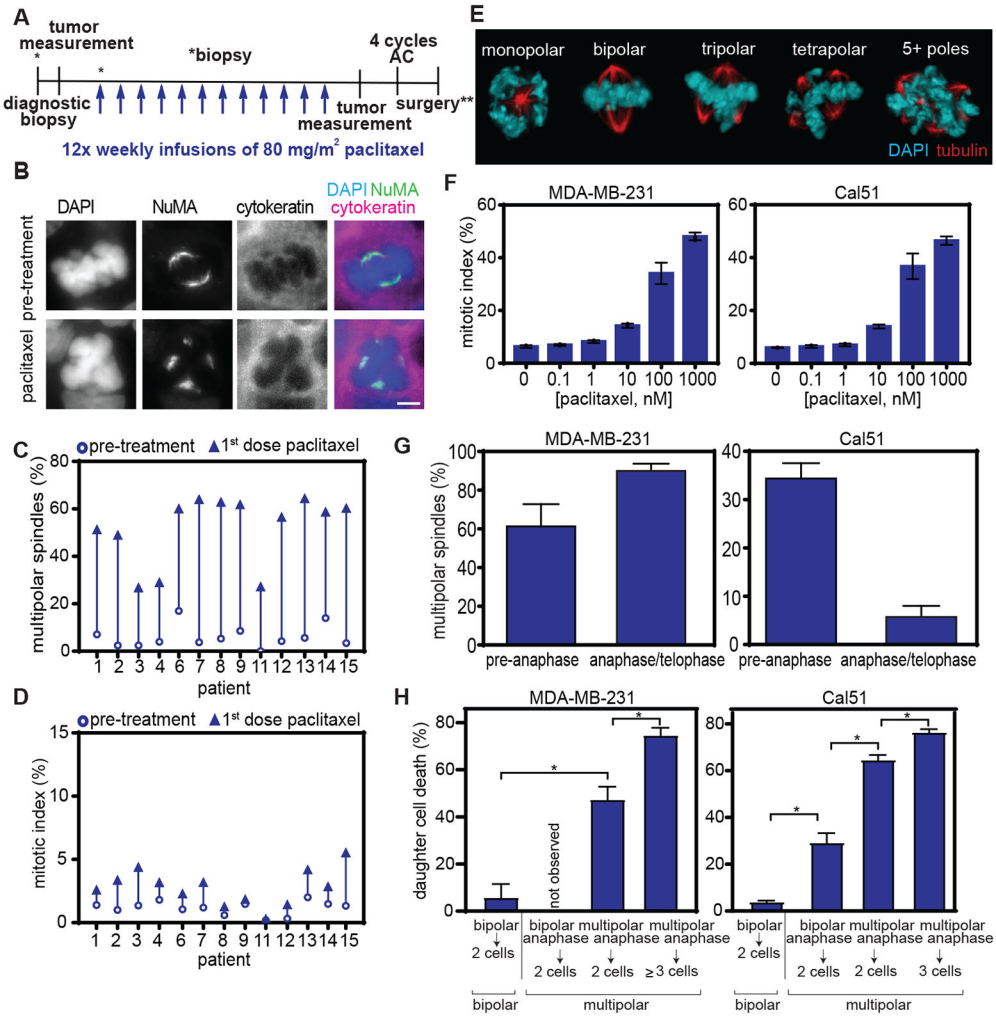

Fig. 1. Clinically relevant concentrations of paclitaxel cause multipolar spindles without mitotic arrest in breast cancer patients and cells.

A) Schematic showing trial design. Research biopsies were obtained prior to paclitaxel treatment and 20 hours after the first dose of paclitaxel. AC = Adriamycin and cyclophosphamide. **indicates that surgery could occur before or after AC, per physician recommendation. **B**) Representative images of bipolar (top) and multipolar (bottom) mitotic cells in patient tumors before and after paclitaxel treatment. Mitotic cells were identified based on DNA morphology and the presence of a mitotic spindle, labeled by Nuclear Mitotic Apparatus protein (NuMA), which localizes to spindle poles. Pan-cytokeratin was used to discriminate between breast epithelial (tumor) cells and stroma. Scale bar, 5 μm. **C-D**) Mitotic effects of 80 mg/m^2 paclitaxel treatment in primary breast cancer patients. Quantification of (**C**) multipolar mitotic spindles, defined as containing >2 NuMA foci, and (**D**) mitotic index before (open circle) and after (arrowhead; the direction indicates increase or decrease) paclitaxel treatment. D, n≥500 cells. For assessment of multipolar spindles in C, mitotic cell sample sizes for patients are 113, 41, 100, 101, 106, 79, 75, 35, 6, 24, 106, 86, and 116 cells, respectively, pre-treatment and 109, 100, 104, 103, 108, 103, 27, 63, 11, 30, 110, 102 and 101 cells, respectively, after treatment. Samples from patients

5 and 10 could not be analyzed due to insufficient tumor tissue collected by biopsy and withdrawal of consent, respectively. **E)** Images of mitotic spindles with the indicated number of poles in MDA-MB-231 cells after treatment with 10 nM paclitaxel. **F**) Quantification of mean mitotic index +/− SEM. n≥300 cells from each of 3 independent experiments. **G)** Quantification of multipolar spindles (mean +/− SD) in Cal51 and MDA-MB-231 cells prior to anaphase onset (n≥100 cells in each of 3 replicates) and in anaphase and telophase (n≥50 cells in each of 3 replicates) in response to 10 nM paclitaxel. **H**) Quantification of percent daughter cell death from long term timelapse microscopy. n≥50 daughter cells in each of 2 replicates. *P<0.05.

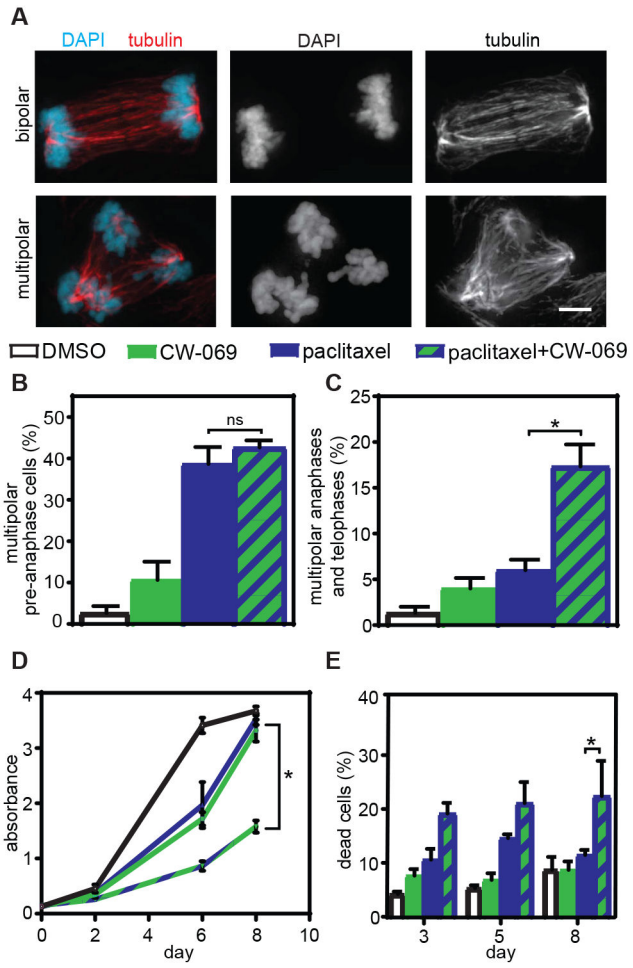

Fig. 2: Elevating the incidence of multipolar divisions in paclitaxel via HSET inhibition increases cytotoxicity.

A) Images of bipolar (top) and multipolar (bottom) anaphase cells. Scale bar, 5 μm.

B-C) Percent of multipolar pre-anaphase, and anaphase/telophase spindles in Cal51 cells following treatment with paclitaxel and the HSET inhibitor CW-069. Mean percentage +/− SEM of mitotic cells with multipolar spindles prior to anaphase (B, n≥ 100 cells in each of 3 replicates) and after anaphase onset (**C**, n≥ 50 anaphase and telophase cells in each of 3 biological replicates). **D-E**) MTT absorbance and percentage of dead cells after treatment of Cal51 cells with paclitaxel and CW-069. **D**) Mean absorbance +/− SEM from MTT viability assays with 10 nM paclitaxel and 50 μM CW-069. n=3. **E**) Mean percentage +/− SEM of dead cells measured by trypan blue exclusion assay. n=3. *P<0.05. ns=not significant.

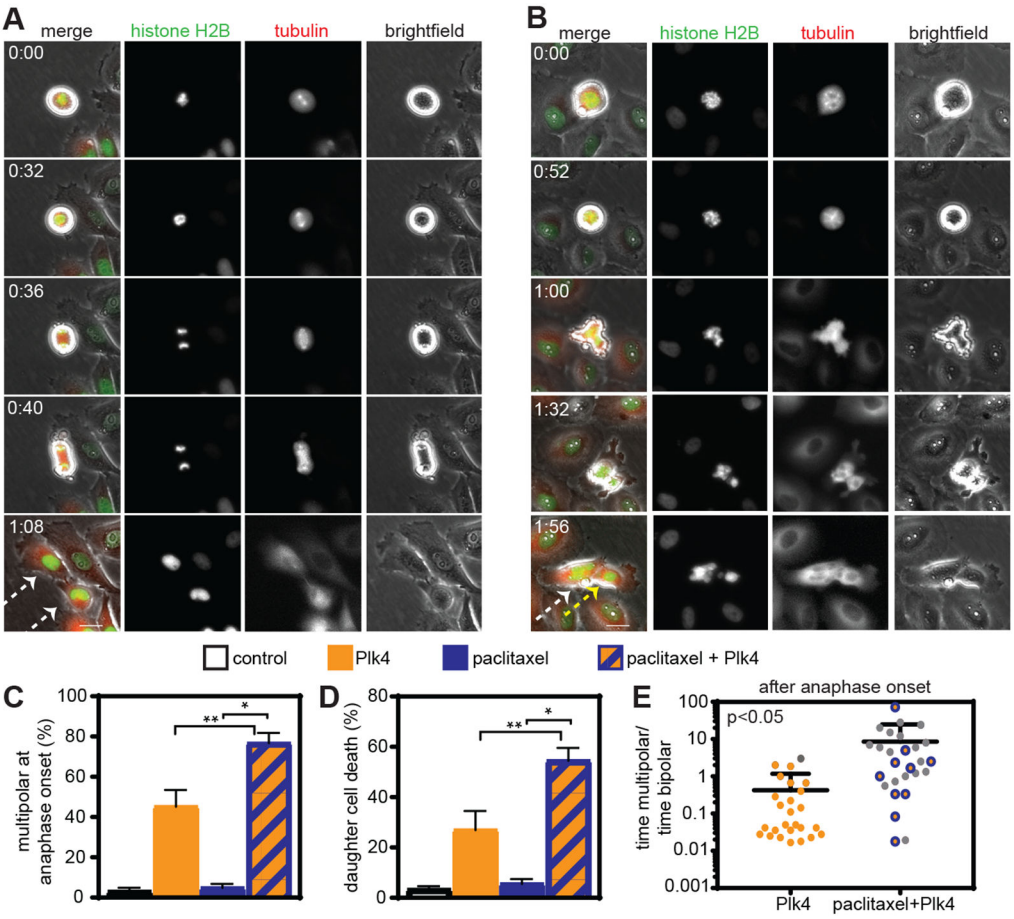

Fig. 3: Increasing the incidence of multipolar divisions through Plk4-induced centriole amplification increases paclitaxel cytotoxicity.

72-hour timelapse analysis of Plk4 inducible MCF10A cells expressing histone H2B-mNeonGreen and mScarlet-tubulin. **A-B**) Still images of (**A**) control cell undergoing bipolar division which produces two viable daughter cells (see Movie S4) and (**B**) Plk4 inducible cell undergoing a multipolar division in the presence of paclitaxel with eventual pole focusing, resulting in the formation of two daughter cells, one of which subsequently dies (see Movie S5). Arrows indicate daughter cells formed after division. White arrows indicate viable daughter cells. Yellow arrow indicates daughter cell that dies after division. Time is indicated in hours:minutes. Scale bar, 5 μm. **C-D**) Quantification of cells observed by timelapse microscopy. **C**) Mean percentage +/− SEM of cells with multipolar spindles at anaphase onset. n=91 control, n=86 paclitaxel, n=95 +doxycycline (Plk4), and n=83 paclitaxel+doxycycline (Plk4) cells from four independent replicates. **D**) Mean percentage of cell death +/− SEM during timelapse. n=167 control, n=111 paclitaxel, n=176 +doxycycline (Plk4), and n=146 paclitaxel+doxycycline (Plk4) daughter cells from four independent replicates. **E**) Ratio of time spent after anaphase onset with a multipolar versus bipolar spindle. Each dot represents a single cell. Gray dots indicate daughter cells that died during the imaging period. **P*<0.05. ***P*<0.001.

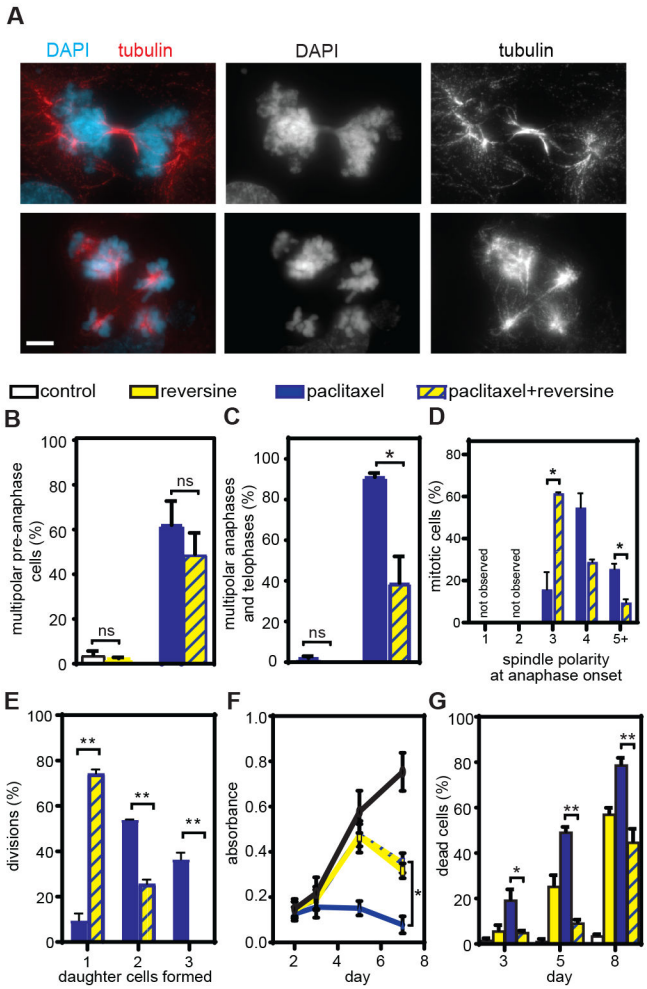

Fig. 4: Reducing multipolar divisions by Mps1 inhibition decreases the cytotoxicity of paclitaxel.

A) Representative images of bipolar (top) and multipolar (bottom) telophase cells. Scale bar, 5 μm. **B**) Percentage (mean +/− SD) of pre-anaphase cells with multipolar spindles in MDA-MB-231 cells upon Mps1 inhibition and paclitaxel tretment. n≥100 cells in each of 3 independent replicates. **C**) Mean percentage +/− SEM of anaphase and telophase cells with multipolar spindles in MDA-MB-231 cells upon Mps1 inhibition and paclitaxel treatment. n≥50 anaphase and telophase cells from each of 3 independent replicates. **D-E**) Quantification of 24 hour timelapse analysis of MDA-MB-231 cells stably expressing RFP-histone H2B and GFP-tubulin at 3 minute intervals. (**D**) Spindle polarity at anaphase onset. Data represent mean +/− SEM of two movies. n=65 and 68 cells in paclitaxel and paclitaxel+reversine conditions, respectively. (**E**). Number of daughter cells formed following mitosis in MDA-MB-231 cells after paclitaxel and reversine treatment. Data represent mean +/− SEM of three movies. n=101 and n=94 divisions in paclitaxel and paclitaxel+reversine conditions, respectively. **F**) Mean absorbance +/− SEM from MTT metabolic viability assay. n=3. **G**) Cell death (mean +/− SEM) in MDA-MB-231 cells following treatment with reversine and paclitaxel, as measured by trypan blue exclusion assay. n=4. *P<0.05. **P<0.001. ns=not significant.

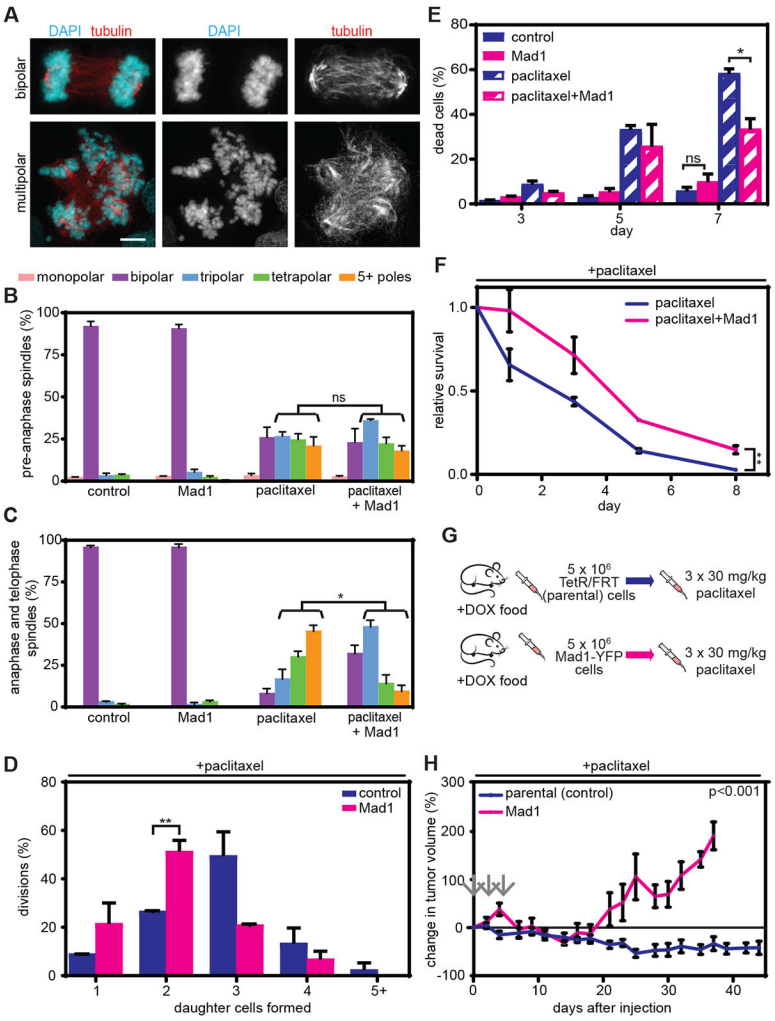

Fig. 5: Reducing multipolar divisions by upregulating Mad1 in MDA-MB-231 cells decreases the cytotoxicity of paclitaxel in vitro and in vivo.

A) Representative images of bipolar (top) and multipolar (bottom) anaphase cells. Scale bar, 5 μm. **B-C**) Cells were treated with vehicle, tet to induce Mad1, 10 nM paclitaxel, or tet and paclitaxel. **B**) Mean +/− SEM of the number of spindle poles in pre-anaphase cells. n≥100 cells from each of 3 replicates. **C**) Mean +/− SEM of spindle pole number in anaphase and telophase cells. n≥50 anaphase and telophase cells in each of 3 independent experiments. **D**) Quantification of the number of daughter cells formed after mitotic division in 10 nM paclitaxel, with and without Mad1 upregulation, assessed by bright-field timelapse microscopy. Data represent the mean +/− SD of two movies. n=65 divisions for paclitaxel alone and n=83 divisions for paclitaxel + Mad1 upregulation. **E**) Mean +/− SEM of cell death, as assessed by trypan blue exclusion assay. n=4. **F**) Relative MTT survival assay (mean +/− SD) over 8 days. n=3. **G**) Schematic of orthotopic experiment. Mice injected with parental or Mad1-YFP inducible MDA-MB-231 cells were treated with 30 mg/kg paclitaxel (gray arrows) every other day for five days once tumors reached a minimum volume of 75 mm^3. **H**) Percent change (mean +/− SEM) in tumor volume after paclitaxel treatment (arrows). n=6 tumors per treatment condition. *=p<0.05. **=p<0.001. ns=not significant.

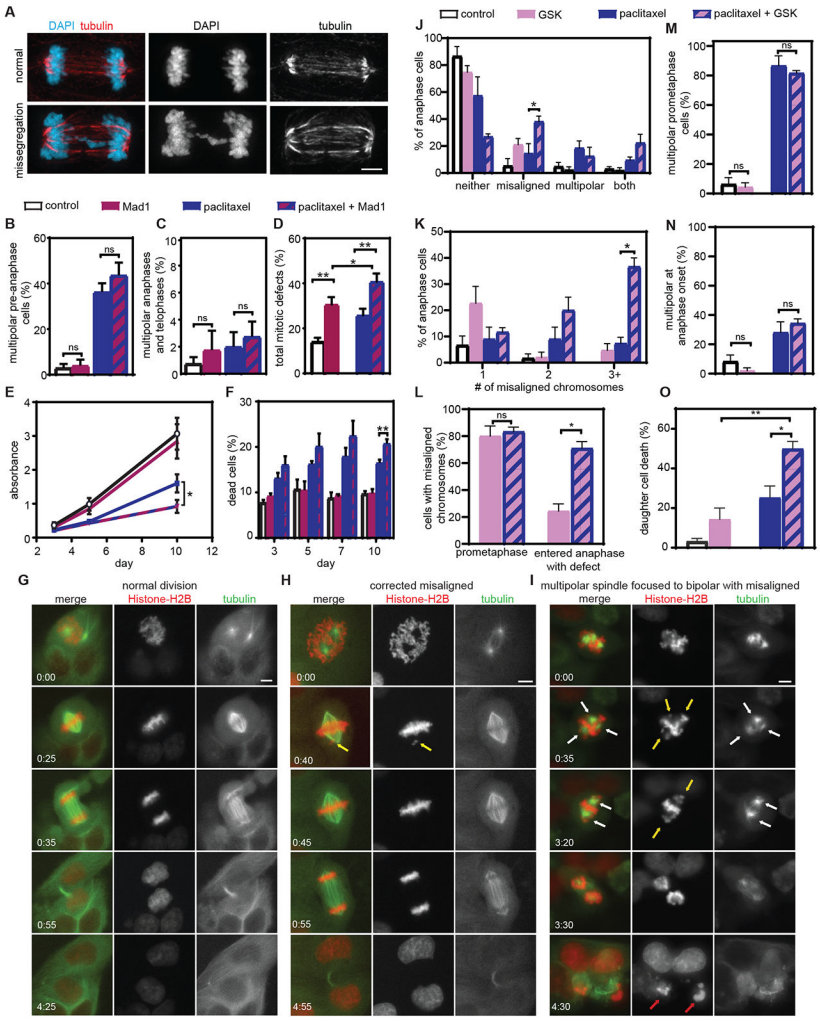

Fig. 6: Increasing chromosomal instability sensitizes Cal51 cells to paclitaxel in vitro.

A) Representative images of a normal bipolar anaphase (top) and a bipolar anaphase with evidence of chromosome missegregation (lagging chromosome, bottom). Scale bar, 5 μm. **B-F**) Cells were treated with vehicle, tet to induce Mad1, 10 nM paclitaxel, or tet and paclitaxel. Mean percentage +/− SEM of multipolar spindles prior to anaphase (**B**, n≥100 cells in each of three biological replicates) and after anaphase onset (**C**, n≥ 50 anaphase and telophase cells in each of three biological replicates). **D**) Quantification of the incidence of total mitotic defects observed by fixed analysis. n≥50 anaphase and telophase cells in each of five biological replicates. **E**) MTT survival assay. Data represent the mean +/− SEM from three biological replicates. **F**) Cell death (mean +/− SEM), measured using trypan blue exclusion assays. n=3. **G-O**) Cal51 cells treated with vehicle, CENP-E inhibitor GSK923295, 5 nM paclitaxel, or both. **G-I**) Still images from timelapse analysis of Cal51 cells with fluorescent chromosomes and microtubules due to endogenous tagging of histone H2B with mScarlet and α-tubulin with mNeonGreen, respectively. Time is indicated in hours:minutes. Scale bar, 5 μm. **G**) Normal bipolar division. **H**) Division in GSK923295, in which a misaligned chromosome, indicated by a yellow arrow, aligns prior to anaphase onset. **I**) Division in combination of 5 nM paclitaxel and 50 nM GSK923295 in which the

prometaphase spindle contains multiple spindle poles (indicated by white arrows), focuses into a bipolar spindle prior to anaphase onset (time 3:20) and enters anaphase in the presence of multiple misaligned chromosomes (yellow arrows). Both daughter cells die by 4:30 (red arrows). **J-N**) Quantitation of mitotic defects at anaphase onset (**J**), number of misaligned chromosomes at anaphase onset (**K**), percentage of cells with misaligned chromosomes in prometaphase and at anaphase onset (**L**), and spindle polarity before (**M**) and at (**N**) anaphase onset. **O**) Percent daughter cell death. Data represent the mean (+/− SEM) from 3 48-hour movies. *$P<0.05$. **$P<0.001$. ns=not significant.

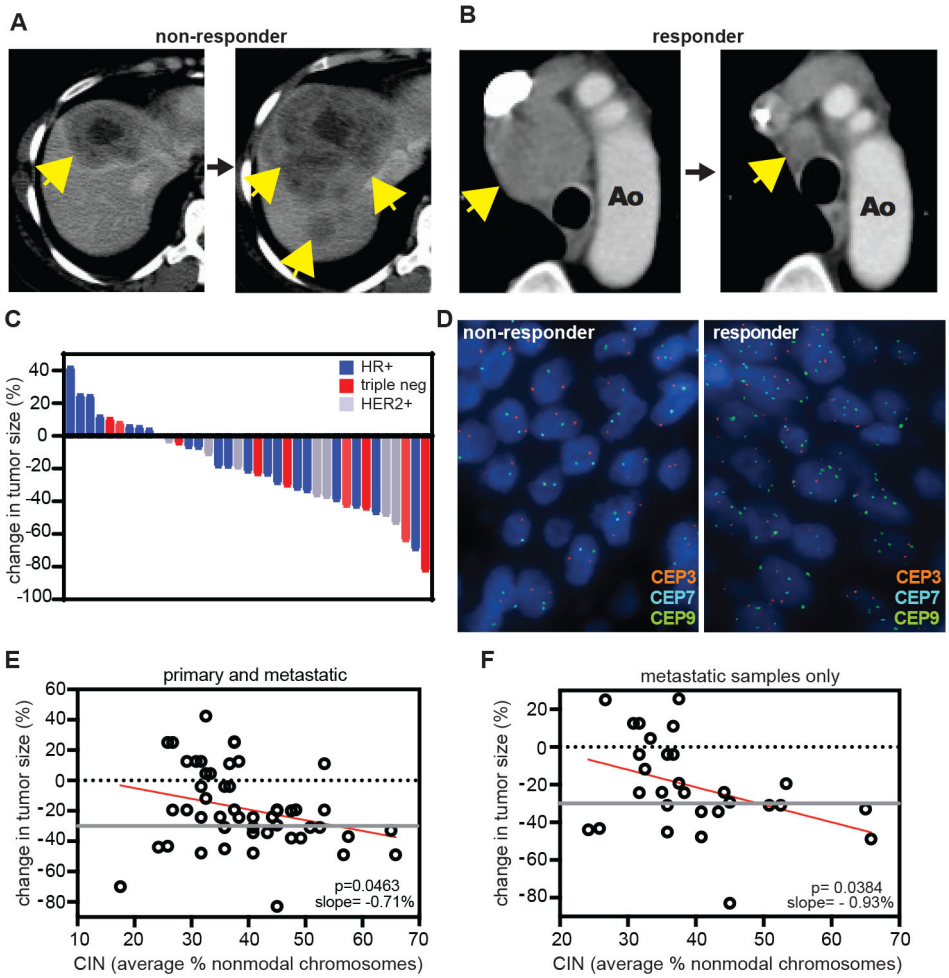

Fig. 7: Pre-treatment chromosomal instability directly correlates with taxane response in metastatic breast cancer patients.

A-B) Representative patient tumor responses to paclitaxel. Yellow arrows indicate tumors. **A**) Progression of a hormone receptor-positive liver metastasis. **B**) Marked improvement of a mediastinal lymph node. **C**) Waterfall plot showing treatment response to taxane therapy in a cohort of 37 metastatic breast cancer patients treated with singleagent taxane. Color indicates breast cancer receptor subtype; hormone receptor positive (HR+), triple negative (triple neg), or human epithelial growth factor receptor 2 positive (HER2+). **D**) Representative FISH images showing probes for centromeres 3, 7, and 9. The average percent non-modal chromosomes was used as a measure of chromosomal instability. **E-F**) Correlation of pre-treatment chromosomal instability with response to taxane treatment. Response cutoff was determined by RECIST 1.1 criteria (26), and is indicated by a gray line. **E**) Data from primary as well as metastatic tumor (51 total) sites. Slope = −0.71%, meaning per percent increase in non-modal chromosomes, tumor size was reduced by an estimated 0.71%. **F**) Data from 29 exclusively metastatic sites. Slope = −0.93%.

Table 1:

Paclitaxel concentration measurements in patient tumors.

Intratumoral and plasma paclitaxel concentrations were measured by HPLC analysis 20 hours after the first dose of paclitaxel. Paclitaxel was quantified per tumor volume. Paclitaxel was not determined (ND) in the tumor biopsies for patients 5 and 12 due to insufficient tumor tissue collected by biopsy. Patient 10 withdrew consent.

Patient	[plasma paclitaxel, μM]	[Intratumoral paclitaxel, μM]	Degree of concentration
1	0.023	1.07	47x
2	0.040	0.34	9x
3	0.030	0.80	27x
4	0.027	0.57	21x
5	0.031	ND	-
6	0.020	3.43	172x
7	0.013	1.55	119x
8	0.011	0.53	48x
9	0.020	0.63	32x
11	0.038	0.57	15x
12	0.040	ND	-
13	0.094	1.67	18x
14	0.048	0.52	11x
15	0.035	1.20	34x